Weierstrass Institute for
Applied Analysis and Stochastics

Numerical reconstruction of elastic obstacles from the far-field data of scattered acoustic waves

J. Elschner, G.C. Hsiao, A. Rathsfeld

Workshop on Inverse Problems for Waves: Methods and Applications

Content

1

1 Direct Problem: Elastic Obstacle in Fluid.

Obstacle and wave.

due to excitation in Ω^c:
determine pressure and
velocity of fluid in Ω^c,
get displacement and
stress of elastic body in Ω,

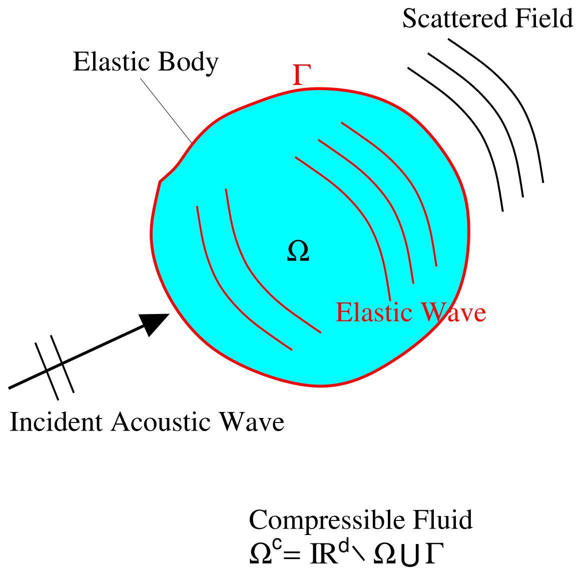

Partial differential equations.

Navier equation, time-harmonic Lamé equ., reduced viscoelastodynamic equ.:

$$\begin{aligned} \Delta^* u(x) + \rho\,\omega^2 u(x) &= 0, \quad x \in \Omega, \\ \Delta^* u(x) &:= \mu\,\Delta u(x) + (\lambda+\mu)\,\nabla\left[\nabla \cdot u(x)\right] \end{aligned}$$

Helmholtz equation for scattered field $p^s = p - p^{\mathrm{inc}}$ ($p^{\mathrm{inc}}(x) := e^{\mathbf{i} k_w \nu \cdot x}$):

$$\Delta p^s(x) + {k_w}^2 p^s(x) = 0, \quad x \in \Omega^c$$

Boundary conditions.

Sommerfeld's radiation condition at infinity for p^s:

$$\frac{x}{|x|} \cdot \nabla p^s(x) - i k_w p^s(x) = o\left(|x|^{-(d-1)/2}\right), \quad |x| \to \infty$$

coupling via transmission condition:

$$\begin{aligned} t(x) &= -\left\{p^s(x) + p^{inc}(x)\right\} n(x), \quad x \in \Gamma \\ \rho_f \omega^2 u(x) \cdot n(x) &= \left\{\frac{\partial p^s(x)}{\partial n} + \frac{\partial p^{inc}(x)}{\partial n}\right\}, \; x \in \Gamma \end{aligned}$$

Indeed: $\rho_f \partial_t^2 \{u(x) e^{-i\omega t}\} \cdot n(x) = ma = F = -\nabla\{p(x) e^{-i\omega t} I\} \cdot n(x)$

Notation.

where traction t:

$$t := t(u) := 2\mu \frac{\partial u}{\partial n}\Big|_\Gamma + \lambda [\nabla \cdot u]\, n\Big|_\Gamma + \mu \begin{cases} n \times [\nabla \times u]\big|_\Gamma & \text{if } d = 3 \\ \begin{pmatrix} n_2(\partial_{x_1} u_2 - \partial_{x_2} u_1) \\ n_1(\partial_{x_2} u_1 - \partial_{x_1} u_2) \end{pmatrix} & \text{if } d = 2 \end{cases}$$

ω frequency ($\omega > 0$)
ρ density of body ($\rho > 0$)
λ, μ Lamé constants ($\mu > 0$, $\lambda + \mu > 0$)
c speed of sound ($c > 0$)
k_w wave number, $k_w^2 = \omega^2 / c^2$
ρ_f density of fluid ($\rho_f > 0$)
n normal at points of Γ exterior w.r.t. Ω

Boundary value problem for partial differential equations, FEM.

Navier in Ω,
Helmholtz in Ω_R,
coupling on Γ,

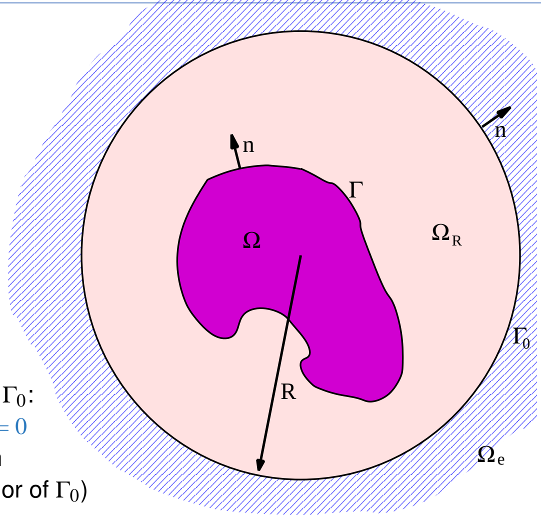

if truncated domain,
then nonlocal condition on Γ_0:
$V^{ac}_{\Gamma_0}[\partial_n p^s] + 0.5 p^s - K^{ac}_{\Gamma_0}[p^s] = 0$
(choose Γ_0 s.t. k_w^2 is not an
eigenvalue of $-\Delta$ on interior of Γ_0)

variational formulation, FEM (cf., e.g., Márquez/Meddahi/Selgas)

Variational formulation. FEM.

$$\mathscr{B}\left(\left(\begin{pmatrix}u\\p^s\\\sigma\end{pmatrix},\begin{pmatrix}v\\q^s\\\chi\end{pmatrix}\right)\right) = -\int_\Gamma p^{inc}n\cdot\overline{v}+\int_\Gamma\frac{\partial p^{inc}}{\partial n}\overline{q^s},$$
$$\forall v\in[H^1(\Omega)]^d,\ q^s\in H^1(\Omega_R),\ \chi\in H^{-1/2}(\Gamma_0)$$

$$\begin{aligned}\mathscr{B}(\dots) \;=\; & \int_\Omega\left\{\lambda\,\nabla\cdot u\,\overline{\nabla\cdot v}+\frac{\mu}{2}\sum_{i,j=1}^{d}\left[\partial_i u_j\overline{\partial_j v_i}+\partial_i u_j\overline{\partial_i v_j}\right]-\rho\omega^2 u\cdot\overline{v}\right\}+\int_\Gamma p^s n\cdot\overline{v}\\ & +\int_{\Omega_R}\left\{\nabla p^s\cdot\overline{\nabla q^s}-k_w{}^2 p\overline{q^s}\right\}+\rho_f\omega^2\int_\Gamma u\cdot n\overline{q^s}-\int_{\Gamma_0}\sigma\overline{q}\\ & +\int_{\Gamma_0}\left\{V^{ac}_{\Gamma_0}\sigma+\left(\frac{1}{2}I-K^{ac}_{\Gamma_0}\right)p^s\right\}\overline{\chi}\end{aligned}$$

Acoustic potentials in nonlocal boundary value condition.

acoustic double and single layer potential operator (two-dimensional case):

$$\begin{aligned}K^{ac}_{\Gamma_0}p^s(x) &:= \int_{\Gamma_0}\frac{\partial G^{ac}(x,y;k_w)}{\partial\nu(y)}p^s(y)\mathrm{d}_{\Gamma_0}y,\\ V^{ac}_{\Gamma_0}\sigma(x) &:= \int_{\Gamma_0}G^{ac}(x,y;k_w)\sigma(y)\mathrm{d}_{\Gamma_0}y,\\ & G^{ac}(x,y;k_w):=\frac{\mathbf{i}}{4}H_0^{(1)}\left(k_w|x-y|\right)\end{aligned}$$

with $H_0^{(1)}$ the Hankel function of the first kind and order zero

Integral equation method. Method of fundamental solutions.

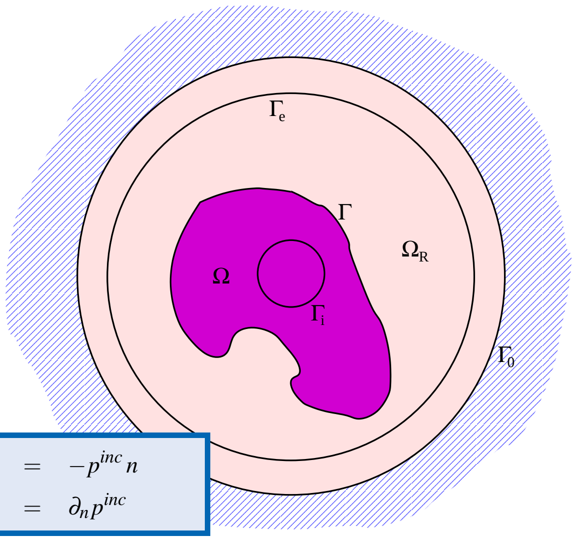

Alternatively,
representation by potentials:

$$\begin{aligned}p &= V^{ac}_{\Gamma_i}\varphi_i\\ u &= V^{el}_{\Gamma_e}\vec{\varphi}_e\end{aligned}$$

Integral equations on Γ:

$$\begin{aligned}tV^{el}_{\Gamma_e}\vec{\varphi}_e+V^{ac}_{\Gamma_i}\varphi_i n &= -p^{inc}n\\ \rho_f\omega^2 n\cdot V^{el}_{\Gamma_e}\vec{\varphi}_e-\partial_n V^{ac}_{\Gamma_i}\varphi_i &= \partial_n p^{inc}\end{aligned}$$

(cf., e.g., Barnett/Betcke for Helmholtz equation)

Elastic potential in integral equation method.

elastic single layer potential operator (two-dimensional case):

$$V^{el}_{\Gamma_e}u(x) := \int_{\Gamma_e}G^{el}(y,x)\vec{\varphi}_e(y)\mathrm{d}_{\Gamma_e}y,$$

with fundamental Green's tensor (Kupradze matrix)

$$G^{el}(x,y) := \frac{1}{\mu}\left(G^{ac}(x,y;k_s)\delta_{ij}+\frac{1}{k_s^2}\frac{\partial^2\left(G^{ac}(x,y;k_s)-G^{ac}(x,y;k_p)\right)}{\partial x_i\partial x_j}\right)^2_{i,j=1}$$

with the compressional wave number $k_s:=\rho\omega^2/(\lambda+2\mu)$ and the shear wave number $k_p:=\rho\omega^2/\mu$

Jones modes.

for exceptional domains (cf. Hargé and Natroshvili/Sadunishvili/Sigua):
$\exists$ eigensolutions = nontrivial solutions of homogeneous equations
$(u,p) = (u_0, 0)$ with Jones mode u_0

$$\boxed{\begin{array}{rcl} \Delta^* u_0(x) + \rho\omega^2 u_0(x) & = & 0,\ x \in \Omega \\ t(u_0)(x) & = & 0,\ x \in \Gamma \\ u_0(x)\cdot n & = & 0,\ x \in \Gamma \end{array}}$$

For example:

$$\boxed{u_0(x_1,x_2) \quad = \quad \frac{1}{\sqrt{x_1^2+x_2^2}}\, J_1\left(\omega\sqrt{\frac{\rho}{\mu}}\sqrt{x_1^2+x_2^2}\right)\begin{pmatrix} -x_2 \\ x_1 \end{pmatrix}}$$

over disc $\Omega = \{x \in \mathbb{R}^2 :\ |x| < r_J\}$, where

J_1 Bessel function of first kind
$r_J := \frac{1}{\omega}\sqrt{\frac{\mu}{\rho}}\, r_J^0$, $r_J^0 := 5.135\,622\,301\,840\,682\,556$,
note that r_J^0 is a root of the transcendental equ. $xJ_1'(x) = J_1(x)$

Example of Jones mode.

real valued x- and y-components of displacement:

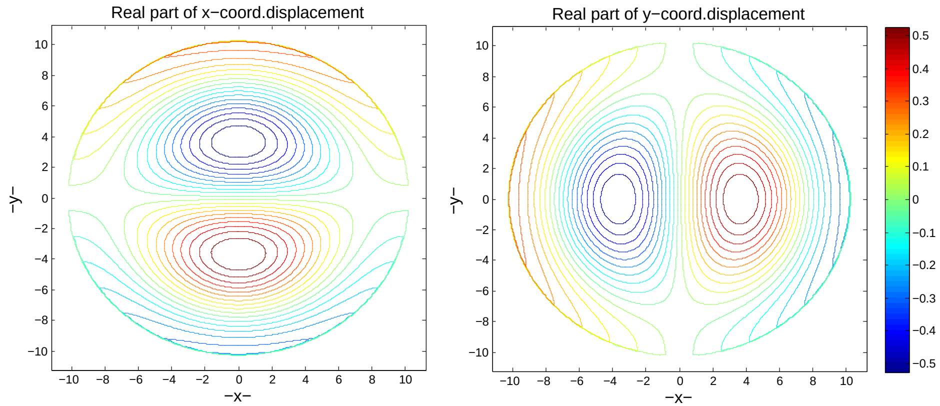

constants: $\omega = 1.5707963267948966$ kHz, $\rho = 6.75\cdot 10^{-8}$ kg/m^3, and
$\mu = 0.66315$ Pa

Far-field pattern.

far-field pattern p^∞:

$$\boxed{\begin{array}{rcl} p^s(x) & = & \dfrac{e^{ik_w|x|}}{|x|^{(d-1)/2}}\, p^\infty\left(\dfrac{x}{|x|}\right) + \mathscr{O}\left(\dfrac{1}{|x|^{(d+1)/2}}\right), \quad |x| \to \infty \\ p^\infty(\hat{x}) & = & c_d \displaystyle\int_{\Gamma_e} \left\{ [ik_w n_y \cdot \hat{x}]\, p(y) + \partial_n p(y) \right\} e^{-ik_w y\cdot\hat{x}} \mathrm{d}y \end{array}}$$

where c_d is a constant ($c_2 = e^{\mathbf{i}\pi/4}/\sqrt{8\pi k_w}$) and where the right-hand side of the last equation is an integral operator with smooth kernel

Example: Non-convex curve.

non-convex curve Γ enclosed by circle Γ_e:

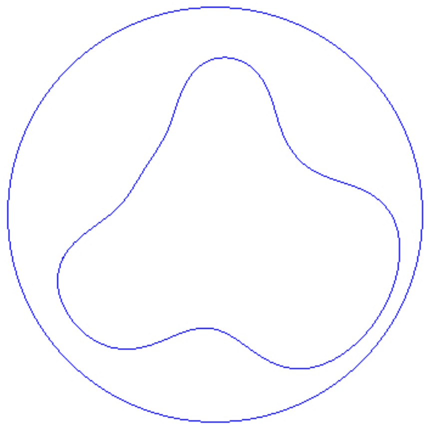

Chosen constants.

frequency	ω	$=$	1.5707963267948966 kHz
density of body	ρ	$=$	$6.75 \cdot 10^{-8}$ kg/m^3
Lamé constant	λ	$=$	1.287373095 Pa
Lamé constant	μ	$=$	0.66315 Pa
speed of sound	c	$=$	1500 m/s
density of fluid	ρ_f	$=$	$2.5 \cdot 10^{-8}$ kg/m^3
direction of incoming plane wave	ν	$=$	$(1,0)^\top$

Pressure.

simulated pressure field:

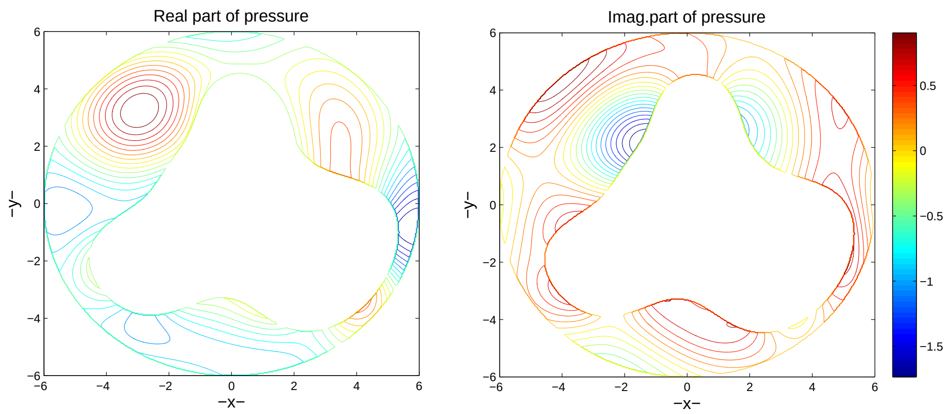

Displacement field.

simulated x-coordinate of displacement field:

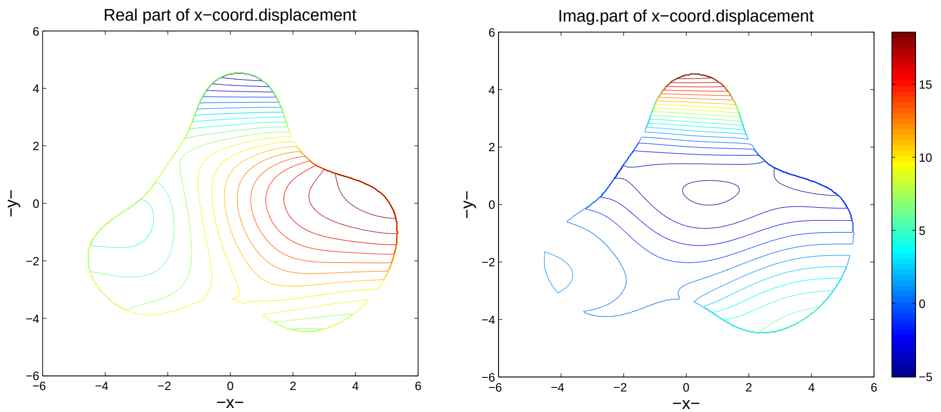

Far field.

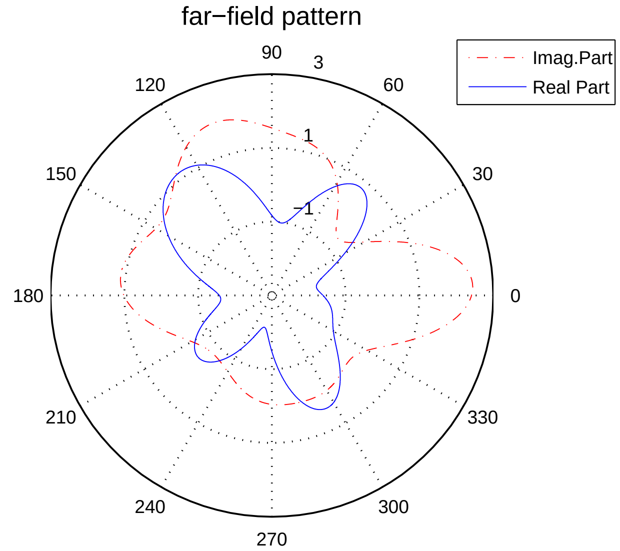

2 Inverse Problem.

Theoretical results.

- Given the far-field pattern p^∞ for all possible directions v of incidence: Find the shape of the obstacle.
  - D. Natroshvili, S. Kharibegashvili, and Z. Tediashvili
    uniqueness for domains:
    - with simply connected complement
    - with parametrizations in $C^{2,\alpha}$, $0 < \alpha \leq 1$

    uniqueness true even in the case of anisotropic elastic obstacle and of generalized Helmholtz equation in the fluid
  - P. Monk and V. Selgas
    uniqueness for domains:
    - with simply connected complement
    - with parametrizations in C^2
    - for which $\nexists$ Jones modes

    uniqueness true even in the case where the Lamé constants depend on the obstacle
- Given the far-field pattern p^∞ for a single or a finite number of incidence directions v: Find the shape of the obstacle.
  - uniqueness problem open

Goals of reconstruction.

Goals for a method based on:
– parametric representation of the boundary curve
– local optimization scheme

- Suppose we know the topology of the obstacle:
  Ω diffeomorphic to ball/disc
- Suppose we know a “good” initial solution.
- Seek a reconstruction with high precision.

- Here, we do not consider alternative methods which determine the topology and work well even if “good” initial solutions are not available: cf. e.g. the sampling method for fluid-solid interaction by Monk/Selgas

Parametrization.

parametrization of star-shaped domain:

$$\boxed{\begin{aligned} \Gamma = \Gamma^{\mathbf{r}} \quad &:= \quad \left\{ \mathbf{r}(\hat{x})\hat{x} : \hat{x} \in \mathbb{S}^{d-1} \right\}, \\ \mathbf{r}\left(e^{i\varphi}\right) \quad &= \quad a_0 + \sum_j \left\{ a_j \cos(j\varphi) + b_j \sin(j\varphi) \right\} \end{aligned}}$$

parametrization to avoid constraint $r_i < \mathbf{r}(\hat{x}) < r_e$:

$$\boxed{\begin{aligned} \Gamma^{\mathbf{r}} \quad &:= \quad \left\{ \widetilde{\mathbf{r}}(\hat{x})\hat{x} : \hat{x} \in \mathbb{S}^{d-1} \right\}, \\ \widetilde{\mathbf{r}}(\hat{x}) \quad &:= \quad \frac{r_e + r_i}{2} + \frac{r_e - r_i}{\pi} \arctan\left(\mathbf{r}(\hat{x})\right) \end{aligned}}$$

Look for unknown boundary of star-shaped domain: $\Gamma \sim \mathbf{r} \sim \{a_j, b_j\}$

Mapping of inverse problem.

fix p^{inc} and consider the mapping

$$\boxed{\begin{array}{rcl} F: H^{2+\varepsilon}(\mathbb{S}^{d-1}) & \longrightarrow & L^2(\mathbb{S}^{d-1}) \\ \Gamma^{\mathbf{r}} = \mathbf{r} & \mapsto & p^\infty \end{array}}$$

where p^∞ is the far-field of p^s and p^s is the pressure part of the solution (u, p^s) to the direct problem including the interface $\Gamma = \Gamma^{\mathbf{r}}$

given: p^∞
find: $\mathbf{r}_{sol}$ s.t. $\boxed{F(\mathbf{r}_{sol}) = p^\infty}$

Lemma (Continuity)

The “curve-to-far field” mapping F is continuous even at boundaries Γ for which there exist Jones modes.

Mapping of inverse problem.

Proof.

- direct problem, boundary/transmission value problem:
  - solution (u, p^s) exists
  - solution (u, p^s) not unique
  - pressure component p^s is unique
- invariant subspace: subspace orthogonal to Jones modes for frequency ω for all frequencies ω': unique solutions in this subspace
  hence, partial solution $(u(\omega'), p^s(\omega'))$ is analytic w.r.t. parameter ω', i.e.,

  $$\boxed{(u(\omega), p^s(\omega)) = \frac{1}{\pi \mathbf{i}} \int_\gamma \frac{1}{\omega' - \omega} (u(\omega'), p^s(\omega'))\, \mathrm{d}\omega'}$$

  with $\omega' \in \gamma$ not a Jones frequency
- pair $(u(\omega'), p^s(\omega'))$ depends continuously on curve Γ ■

3

3 Reduction to Optimization Problems.

Equivalent optimization problem.

first equivalent optimization problem:

find least-squares solution $\mathbf{r}_{min}$ which is a minimizer of the following optimization problem:

$$\boxed{\begin{array}{c} \inf_{\mathbf{r} \in H^{2+\varepsilon}(\mathbb{S}^{d-1})} \mathscr{J}(\mathbf{r}) \\ \mathscr{J}(\mathbf{r}) := \|F(\mathbf{r}) - p^\infty\|^2_{L^2(\mathbb{S}^{d-1})} \end{array}}$$

“Equivalent” optimization problem.

first “equivalent” optimization problem:

find approximate solution $\mathbf{r}_{min}$ which is a minimizer of the following optimization problem:

$$\inf_{\mathbf{r}\in H^{2+\varepsilon}(\mathbb{S}^{d-1})} \mathscr{J}_{\gamma}(\mathbf{r})$$

$$\mathscr{J}_{\gamma}(\mathbf{r}) := \|F(\mathbf{r}) - p^{\infty}_{noisy}\|^2_{L^2(\mathbb{S}^{d-1})} + \gamma\|\mathbf{r}\|^2_{H^{2+\varepsilon}(\mathbb{S}^{d-1})}$$

where γ is a small regularization parameter

Suppose $\|p^{\infty} - p^{\infty}_{noisy}\|^2_{L^2(\mathbb{S}^{d-1})} < const.\gamma$

Next “equivalent” optimization problem.

second “equivalent” optimization problem:

find approximate solution $(\mathbf{r}_{min}, u_{min}, p_{min})$ which is a minimizer of the following optimization problem:

$$\inf_{\mathbf{r}\in H^{2+\varepsilon}(\mathbb{S}^{d-1}), u\in[H^1]^d, p\in H^1} \mathscr{J}_{\gamma}(\mathbf{r},u,p)$$

$$\begin{aligned}\mathscr{J}_{\gamma}(\mathbf{r},u,p) \quad := \quad & \|\text{far-field}(p) - p^{\infty}_{noisy}\|^2_{L^2(\mathbb{S}^{d-1})} + \\ & \|\Delta^* u + \ldots - 0\|^2 + \|\Delta p + \ldots - 0\|^2 + \\ & \|t(u) + pn + \ldots\|^2 + \|u\cdot n - \ldots\|^2 + \\ & \|V(\partial_n p|_{\Gamma_0}) + \ldots\|^2 + \\ & \gamma\|\mathbf{r}\|^2_{H^{2+\varepsilon}(\mathbb{S})} + \gamma\|u\|^2_{[H^1]^d} + \gamma\|p\|^2_{H^1}\end{aligned}$$

where γ is a small regularization parameter

Last “equivalent” optimization problem.

third “equivalent” optimization problem:

fix Γ_e and Γ_i and find approximate solution $(\mathbf{r}_{min}, \varphi_{i,min}, \vec{\varphi}_{e,min})$ which is a minimizer of the following optimization problem:

$$\inf_{\mathbf{r}\in H^{2+\varepsilon}(\mathbb{S}^{d-1}), \varphi_i\in H^{-1}(\Gamma_i), \vec{\varphi}_e\in[H^{-1}(\Gamma_e)]^d} \mathscr{J}_{\gamma}(\mathbf{r},\varphi_i,\vec{\varphi}_e)$$

$$\begin{aligned}\mathscr{J}_{\gamma}(\mathbf{r},\varphi_i,\vec{\varphi}_e) \quad := \quad & c\left\|\text{far-field}\left(V^{ac}_{\Gamma_i}\varphi_i\right) - p^{\infty}_{noisy}\right\|^2_{L^2(\mathbb{S}^{d-1})} + \\ & \left\|tV^{el}_{\Gamma_i}\vec{\varphi}_e + V^{ac}_{\Gamma_i}\varphi_i n + p^{inc} n\right\|^2 + \\ & \left\|\rho_f\omega^2 n\cdot V^{el}_{\Gamma_i}\vec{\varphi}_e - \partial_n V^{ac}_{\Gamma_i}\varphi_i - \partial_n p^{inc}\right\|^2 + \\ & \gamma\|\varphi_i\|^2_{H^{-1}(\Gamma_i)} + \gamma\|\vec{\varphi}_e\|^2_{[H^{-1}(\Gamma_e)]^d}\end{aligned}$$

where γ is a small regularization parameter

Comparison of three approaches.

- first method:
  - smallest number of optimization parameters
  - complicated objective functional
  - computation of objective functional requires solution of direct problem
  - we have implemented this FEM based Newton iteration using
    - grid generator “netgen” (cf. Schöberl)
    - solver “pardiso” (cf. Schenk/Gärtner/Fichtner)
- second method:
  - huge set of optimization parameters
  - solution of direct problem not needed (good if $\exists$ Jones mode)
  - not implemented
- third method:
  - large but not huge set of optimization parameters
  - solution of direct problem not needed (good if $\exists$ Jones mode)
  - additional difficulties due to ill-posed potential representation
  - possible: advanced algorithm with Γ_i and Γ_e updated during iteration process (compare, e.g., You/Miao/Liu & Ivanyshyn/Kress/Serranho)
  - we have implemented this Kirsch-Kress algorithm

Convergence of FEM based Newton iteration.

$$\mathscr{J}_\gamma(\mathbf{r}) = \|F(\mathbf{r}) - p^\infty_{noisy}\|^2_{L^2(\mathbb{S}^{d-1})} + \gamma\|\mathbf{r}\|^2_{H^{2+\varepsilon}(\mathbb{S}^{d-1})} \longrightarrow \min$$

Theorem (FEM based Newton iteration)

Assume the noise satisfies $\|p^\infty - p^\infty_{noisy}\|^2_{L^2(\mathbb{S}^{d-1})} < constant\ \gamma$.

i) $\forall \gamma > 0$: $\exists$ *minimizer* $\mathbf{r}^\gamma_{noisy}$ *of optimization problem.*

ii) $\gamma \to 0$: $\mathscr{J}_\gamma(\mathbf{r}^\gamma_{noisy}) \to \inf_{\mathbf{r}\in H^{2+\varepsilon}(\mathbb{S}^{d-1})} \mathscr{J}_0(\mathbf{r})$

iii) *Suppose* $\exists$ *solution* $\mathbf{r}^*$:

$\exists$ *subsequence* $\mathbf{r}^{\gamma_n}_{noisy}$ *such that*

a) $\mathbf{r}^{\gamma_n}_{noisy} \to \mathbf{r}^{**}$ *strongly in* $H^{2+\varepsilon/2}(\mathbb{S}^{d-1})$ *for* $n \to \infty$

b) $\mathbf{r}^{\gamma_n}_{noisy} \to \mathbf{r}^{**}$ *weakly in* $H^{2+\varepsilon}(\mathbb{S}^{d-1})$ *for* $n \to \infty$

c) $F(\mathbf{r}^{**}) = p^\infty$

iv) *Suppose* $\exists$ *unique solution* $\mathbf{r}^*$:

a) $\mathbf{r}^\gamma_{noisy} \to \mathbf{r}^*$ *strongly in* $H^{2+\varepsilon/2}(\mathbb{S}^{d-1})$ *for* $\gamma \to 0$

b) $\mathbf{r}^\gamma_{noisy} \to \mathbf{r}^*$ *weakly in* $H^{2+\varepsilon}(\mathbb{S}^{d-1})$ *for* $\gamma \to 0$

Convergence of Kirsch-Kress algorithm.

$$\mathscr{J}_\gamma(\mathbf{r},\varphi_i,\vec{\varphi}_e) \quad := \quad c\|\text{far-f.}\,(V^{ac}_{\Gamma_i}\varphi_i) - p^\infty_{noisy}\|^2 + \|\text{transm.cond.}(V^{ac}_{\Gamma_i}\varphi_i, V^{el}_{\Gamma_e}\vec{\varphi}_e)|_{\Gamma^r}\|^2 + \gamma\|\varphi_i\|^2 + \gamma\|\vec{\varphi}_e\|^2 \quad \longrightarrow \min$$

Theorem (Kirsch-Kress algorithm)

Assume:

- *There is a solution* $\mathbf{r}^*$.
- *The number* k^2 *is not a Dirichlet eigenvalue for* $-\Delta$ *in interior of* Γ_i.
- *The noise satisfies* $\|p^\infty - p^\infty_{noisy}\|^2_{L^2(\mathbb{S}^{d-1})} < constant\ \gamma$.

Then: **i)** $\forall \gamma > 0$: $\exists$ *minimizer* $(\mathbf{r}^\gamma_{noisy}, \varphi^\gamma_{i,noisy}, \vec{\varphi}^\gamma_{e,noisy})$ *of optimization problem.*

ii) $\gamma \to 0$: $\mathscr{J}_\gamma(\mathbf{r}^\gamma_{noisy}, \varphi^\gamma_{i,noisy}, \vec{\varphi}^\gamma_{e,noisy}) \to \inf_{\mathbf{r},\varphi_i,\vec{\varphi}_e} \mathscr{J}_0(\mathbf{r},\varphi_i,\vec{\varphi}_e)$

iii) $\exists$ *subsequence* $\mathbf{r}^{\gamma_n}_{noisy}$ *such that*

a) $\mathbf{r}^{\gamma_n}_{noisy} \to \mathbf{r}^{**}$ *strongly in* $H^{2+\varepsilon/2}(\mathbb{S}^{d-1})$ *for* $n \to \infty$

b) $\mathbf{r}^{\gamma_n}_{noisy} \to \mathbf{r}^{**}$ *weakly in* $H^{2+\varepsilon}(\mathbb{S}^{d-1})$ *for* $n \to \infty$

c) $F(\mathbf{r}^{**}) = p^\infty$

iv) *Suppose* $\exists$ *unique solution* $\mathbf{r}^*$:

a) $\mathbf{r}^\gamma_{noisy} \to \mathbf{r}^*$ *strongly in* $H^{2+\varepsilon/2}(\mathbb{S}^{d-1})$ *for* $\gamma \to 0$

b) $\mathbf{r}^\gamma_{noisy} \to \mathbf{r}^*$ *weakly in* $H^{2+\varepsilon}(\mathbb{S}^{d-1})$ *for* $\gamma \to 0$

Convergence of Kirsch-Kress algorithm.

Proof.

$$\boxed{\begin{gathered}\mathscr{B}: \begin{pmatrix}\vec{\varphi}_e\\ \varphi_i\end{pmatrix} \mapsto \begin{pmatrix} tV^{el}_{\Gamma_i}\vec{\varphi}_e + V^{ac}_{\Gamma_i}\varphi_i n \\ \rho_f\omega^2 n\cdot V^{el}_{\Gamma_i}\vec{\varphi}_e - \partial_n V^{ac}_{\Gamma_i}\varphi_i\end{pmatrix}\\ \mathscr{B}:\ [L^2(\Gamma_e)]^d \times L^2(\Gamma_i) \longrightarrow [L^2(\Gamma)]^d \times L^2(\Gamma)\end{gathered}}$$

Essential lemma: The image $\operatorname{im}\mathscr{B}$ of operator $\mathscr{B}$ is dense in the subspace

$$\boxed{\left\{(\vec{\varphi},\varphi)^\top \in [L^2(\Gamma)]^d \times L^2(\Gamma):\ \langle\vec{\varphi},u_0\rangle = 0,\ \forall\, u_0 \text{ Jones mode}\right\}.}$$

∎

Derivatives and Quadrature.

Derivatives for gradient based optimization schemes

- derivatives for FEM based Newton method:
  - shape optimization techniques
  - get gradients by solving the FEM system of the direct problem with new right-hand side
  - 2D case: direct solver with LU factorization
- derivatives for Kirsch-Kress method:
  - reduces to simple differentiation of Green's kernels
  - fourth order derivatives of Helmholtz kernel

Quadratures for Kirsch-Kress method

- no quadrature!
  - layer functions φ_i and $\vec{\varphi}_e$ in $H^{-1}(\Gamma_i)$ and $[H^{-1}(\Gamma_e)]^2$, respectively
  - layer functions φ_i and $\vec{\varphi}_e$: linear combinations of Dirac δ functions

Optimization algorithm.

Which optimization scheme?

- FEM based Newton method:
  - small number of parameters
  - Gauss-Newton method
- Kirsch-Kress method:
  - larger number of parameters
  - conjugate gradient method (nonlinear variant)
  - Gauss-Newton and Levenberg-Marquardt method: solve linear systems of dimension larger than those of the direct solver

Scaling.

Scaling of optimization scheme

- number of necessary iteration depends on conditioning of optimization problem
- natural scaling
  - scale far-field values in accordance with measurement uncertainties
  - scale parameters in accordance with the reconstruction requirements
- scaling for a fast iterative solution adapted in accordance with numerical tests
  - calibration constants before the several terms of the objective functional (e.g. constant c and regularization parameter γ)
  - replace optimization parameters by multiple of parameters in order to get gradients with components of equal size

$$\boxed{\mathbf{r} = \mathbf{r}/c_{\mathbf{r}}, \quad \varphi_i = \varphi_i/c_i, \quad \vec{\varphi}_e = \vec{\varphi}_e/c_e}$$

4

4 Numerical Tests.

Reconstruction of egg domain.

initial solution and egg domain:

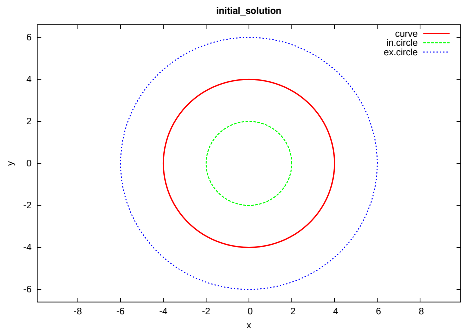

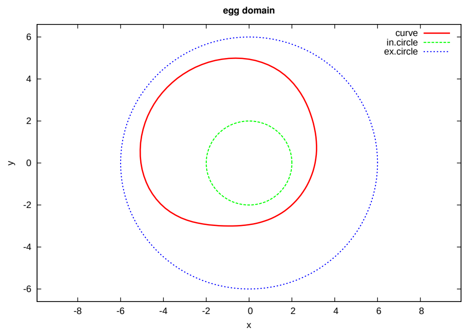

Fourier coefficients:

$$\begin{array}{llllll} a_0 = 0 & & & & \\ a_1 = -1 & a_2 = 0.1 & a_3 = 0.01 & a_4 = -0.001 & a_5 = 0.0001 \\ b_1 = 1 & b_2 = 0.1 & b_3 = 0.01 & b_4 = 0.001 & b_5 = 0.0001 \end{array}$$

Reconstruction of non-convex domain.

initial solution and non-convex domain:

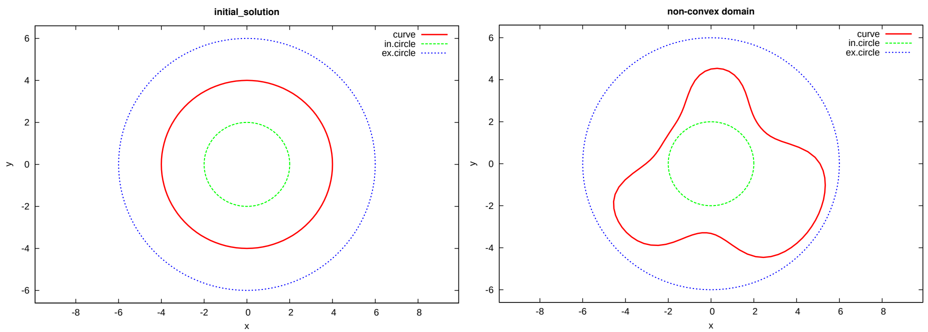

Fourier coefficients:

$$\begin{array}{llllllll} a_0 = & 0 & & & & & & \\ a_1 = & 1 & a_2 = & 0.10 & a_3 = & 0.04 & a_4 = & 0.016 & a_5 = 0.008 \\ b_1 = & -1 & b_2 = & 0.02 & b_3 = & -1.500 & b_4 = & -0.010 & b_5 = 0.008 \end{array}$$

Data and Scaling.

far-field data:

- simulated far-field data
- computed in 80 uniformly distributed direction
- FEM computation over finer FEM triangulation (meshsize smaller at least by factor 0.25)

scaling:

- for Kirsch-Kress method with 44 discretization points on each curve: $c = 4000$, $c_{\mathbf{r}} = 1$, $c_i = 0.1$, $c_e = 0.005$

Reconstruction results.

Results:

- Good reconstruction with FEM based Newton method for both domains even without regularization terms ($\gamma = 0$)
- Good reconstruction with Kirsch-Kress method for egg domain
- No reconstruction with Kirsch-Kress method for non-convex domain
  - Regularized solution of direct problem obtained with the Tikhonov term in our optimization scheme is bad
  - Regularization with truncated SVD representation and for a suitable very small range of regularization parameters: reasonable regularized solution of direct problem
  - Inverse crime (compute far-field data via integral equations): Good reconstruction with Kirsch-Kress method for non-convex domain
- Good reconstruction with Kirsch-Kress method for non-convex domain if curves Γ_i and Γ_e are close to unknown curve Γ

Reconstruction by FEM based Newton method.

Convergence of FEM based Newton

far-field data simulated by FEM computation on higher level:
reconstruction error $\mathbf{err} := \|\mathbf{r} - \mathbf{r}_{FEM}\|_{L^\infty}$ and number of iterations $\mathbf{it}$ depending on meshsize $\mathbf{h}$ of FEM discretization

h	err	it
	1.2596	0
0.5	0.0759	6
0.25	0.0247	8
0.125	0.00876	8
0.0625	0.00329	10
0.03125	0.00156	10

egg domain

h	err	it
	1.5733	0
0.25	1.1435	20
0.125	0.00924	17
0.0625	0.00401	15
0.03125	0.00157	18

non-convex domain

Reconstruction by Kirsch-Kress method for egg domain.

Different optimization schemes for Kirsch-Kress method

Method of conjugate gradients: too slow or different limit
Gauss-Newton method with regularization: GNw
Levenberg-Marquardt method with regularization: LMw
Levenberg-Marquardt method “without” regularization: LMo
(code and standard choice of parameters by M. Lourakis)

pnts. on Γ	γ	GNw		LMw		LMo	
		1.2596	(0)	1.2596	(0)	1.2596	(0)
22	$4 \cdot 10^{-8}$	0.05427	(13)	0.05461	(30)	0.06793	(30)
44	$2.5 \cdot 10^{-13}$	0.002136	(13)	0.002007	(320)	0.002095	(320)
88	$4 \cdot 10^{-14}$	0.0002126	(13)	0.0002107	(80)	0.0001997	(160)

Error $||\mathbf{r} - \mathbf{r}_{KK}||_{L^\infty}$ and number of iterations for Kirsch-Kress method egg domain

Reconstruction by Kirsch-Kress method for non-convex domain.

initial solution and non-convex domain:

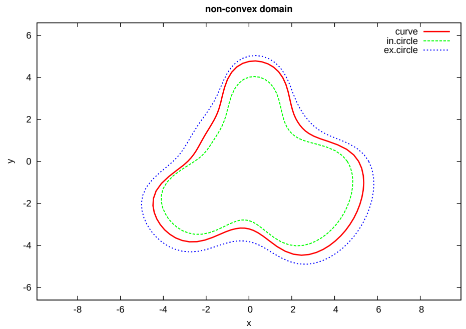

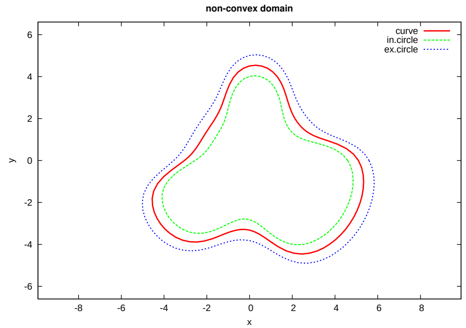

For $\gamma = 10^{-8}$, $c = 10\,000$, $c_{\mathbf{r}} = 1$, $c_i = 1$, $c_e = 0.2$, and 352 discretization points on each curve:

initial deviation of radial functions: 0.296
number of iterations: 11
reconstruction error: $0.000\,279$

Reconstruction by Kirsch-Kress method for non-convex domain.

- What shall we do with an initial solution like the disc?
- curves Γ_i and Γ_e must be close to iterative solution: update Γ_i and Γ_e during the iterative solution process
  - choose Γ_i and Γ_e by their radial functions:

    $$\boxed{\begin{aligned} \mathbf{r}_i &= \mathbf{r} - \frac{1}{2} \\ \mathbf{r}_e &= \mathbf{r} + \frac{1}{2} \end{aligned}}$$

    with $\mathbf{r}$ the radial function of the last iterative solution $\Gamma = \Gamma^{\mathbf{r}}$
    - $*$ Note that this is the setting for which the Kirsch-Kress method is convergent according to the previous test!
  - for fixed Γ_i and Γ_e: perform one step of Gauss-Newton method, but reduce the iteration step s.t. solution curve remains between Γ_i and Γ_e
  - if the iteration step remains small: fix Γ_i and Γ_e and perform more Gauss-Newton steps

Reconstruction by Kirsch-Kress method for non-convex domain.

1st step: initial solution and first iterate of Gauss-Newton method

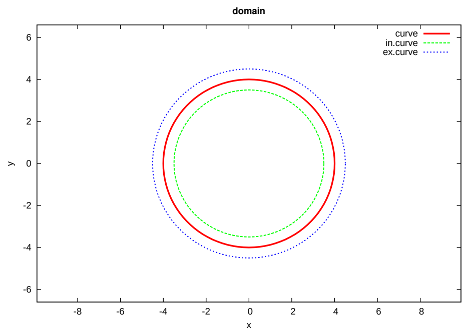

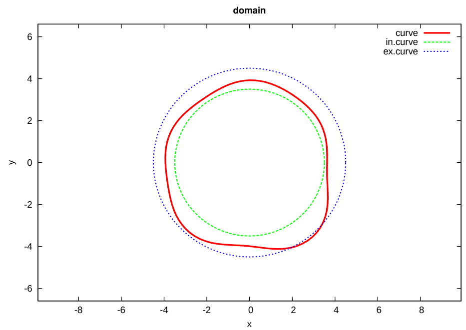

Reconstruction by Kirsch-Kress method for non-convex domain.

2nd step: initial solution and first iterate of Gauss-Newton method

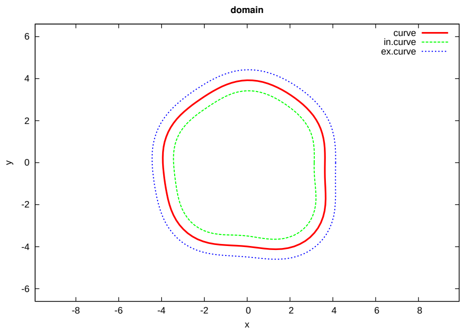

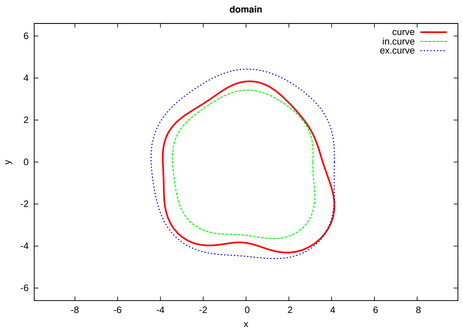

Reconstruction by Kirsch-Kress method for non-convex domain.

3rd step: initial solution and first iterate of Gauss-Newton method

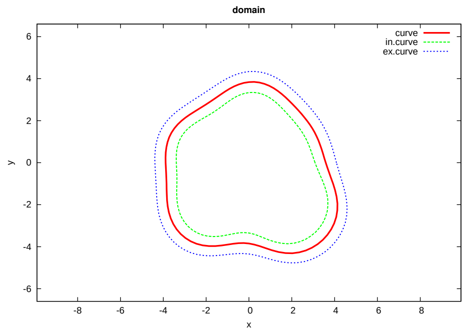

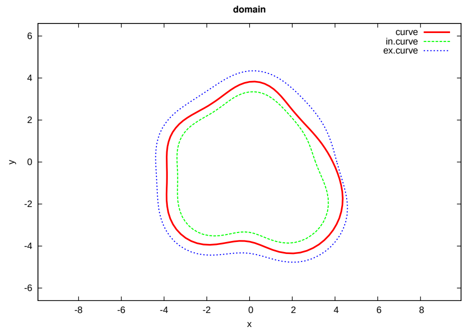

Reconstruction by Kirsch-Kress method for non-convex domain.

4th step: initial solution and first iterate of Gauss-Newton method

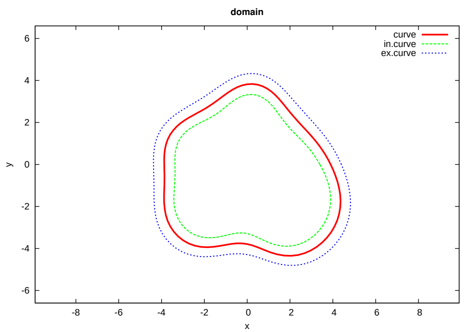

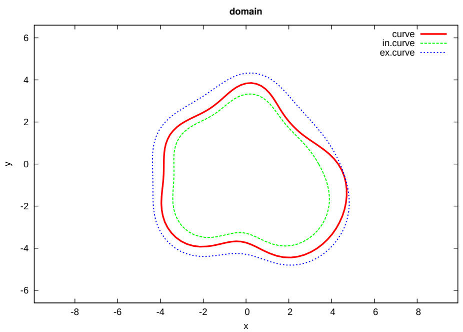

Reconstruction by Kirsch-Kress method for non-convex domain.

5th step: initial solution and first iterate of Gauss-Newton method

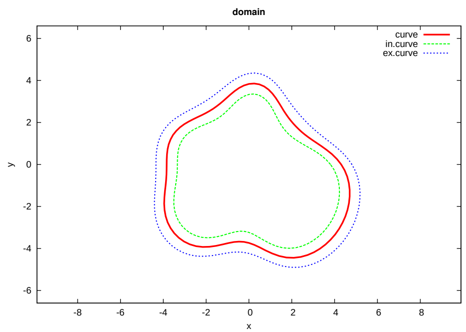

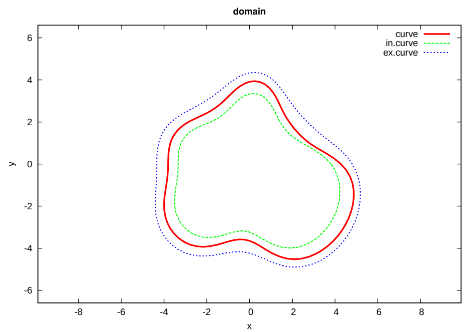

Reconstruction by Kirsch-Kress method for non-convex domain.

6th step: initial solution and first iterate of Gauss-Newton method

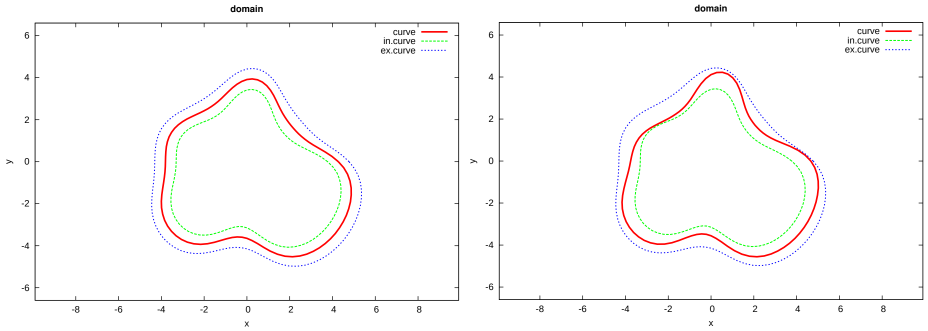

Reconstruction by Kirsch-Kress method for non-convex domain.

7th step: initial solution and first iterate of Gauss-Newton method

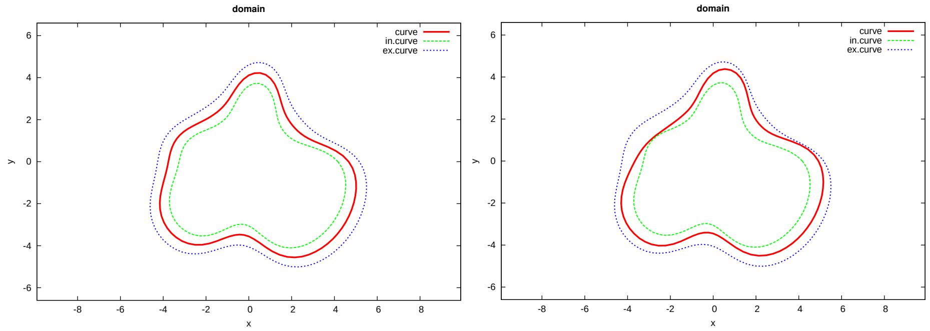

Reconstruction by Kirsch-Kress method for non-convex domain.

8th step: initial solution and first iterate of Gauss-Newton method

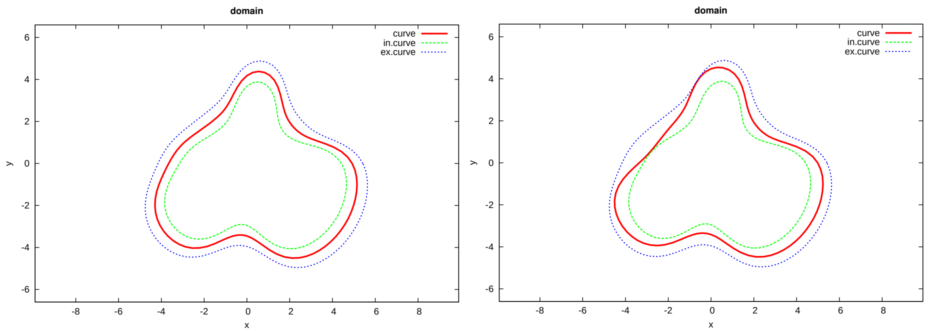

Reconstruction by Kirsch-Kress method for non-convex domain.

9th step: initial solution and first iterate of Gauss-Newton method

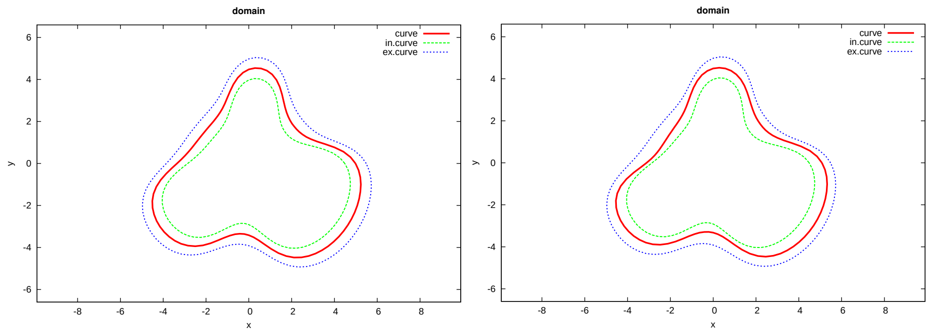

Reconstruction by Kirsch-Kress method for non-convex domain.

Last step: 10 Gauss-Newton iterations

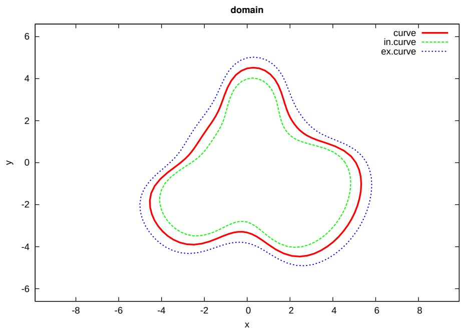

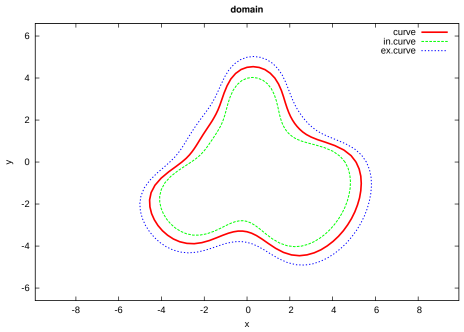

Reconstruction of curve with 14 Fourier coefficients.

Curve with 14 Fourier coefficients: Reconstruction with only 10 coefficients.

- additional non-zero coefficients for the non-convex domain: $a_6 = 0.004$, $a_7 = 0.001$, $b_6 = -0.004$, and $b_7 = 0.001$
- radial deviation of curve with 14 Fourier non-zero coefficients to curve with 10 is 0.0075
- initial solution $a_i^{ini} = 0.75\, a_i$ (for $a_i^{ini} = 0$: convergence only for $h = 0.03125$)

h	err	it
	1.57	0
0.5	0.1147	7
0.25	0.03812	8
0.125	0.01878	7
0.0625	0.01688	7
0.03125	0.01678	7

FEM based Newton iteration for non-convex domain with 14 coefficients

Kirsch-Kress method for Γ_i and Γ_e close to Γ: reduces radial deviation error to 0.00898 after 12 iteration

Noisy data.

Perturbation of far-field data

perturbed far-field data of egg domain: Add random number uniformly distributed in $[-\varepsilon, \varepsilon]$

ε	$\|\|\mathbf{r} - \mathbf{r}_{FEM}\|\|_{L^\infty}$
0.	0.001 568
0.001	0.002 637
0.005	0.007 156
0.01	0.013 68
0.05	0.054 33
0.1	0.108 7

FEM with stepsize 0.03125

ε	γ	$\|\|\mathbf{r} - \mathbf{r}_{KK}\|\|_{L^\infty}$
0.	$2.5 \cdot 10^{-13}$	0.002 136
0.0001	$2.5 \cdot 10^{-11}$	0.003 640
0.001	$2.5 \cdot 10^{-8}$	0.020 41
0.003	$2.5 \cdot 10^{-7}$	0.056 86
0.005	$1 \cdot 10^{-6}$	0.099 97

Kirsch-Kress with 44 points on Γ

Reconstruction of domain with Jones modes.

initial solution and non-convex domain:

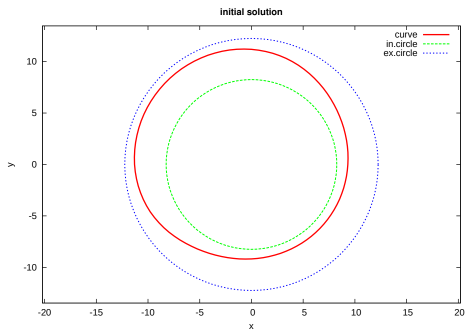

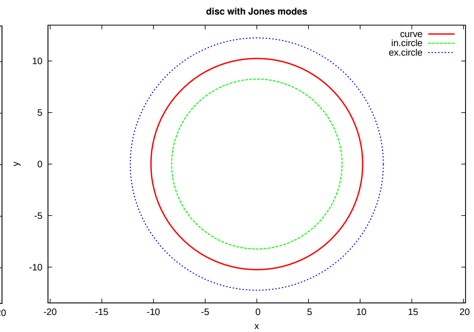

- Kirsch-Kress algorithm:
  - nmb.discr.pnts. 176, $\gamma = 4 \cdot 10^{-14}$, $c = 200$, $c_{\mathbf{r}} = 1$, $c_i = 5$, $c_e = 0.05$
  - initial deviation 1.26, 8 iterations, reconstruction error $0.000\,814$
- FEM based Newton iteration:
  - direct solver “pardiso” yields partial solution of variational system,
  - initial deviation 1.26, 13 iterations, reconstruction error $0.000\,492$

5 Conclusions.

Conclusions.

- Advantage of Kirsch-Kress method:
  - high accuracy of reconstruction.
  - fast computation.
- Disadvantages of Kirsch-Kress method:
  - sensitive to small perturbations of the far-field data.
  - sensitive to scaling of optimization problem: a lot of parameters to be adapted.
  - ill-posed integral equations: The Kirsch-Kress method does not require the solution of the direct problem. However, it works only if the direct problem is solvable by the ill-posed integral equations. To decrease the ill-posedness, the outer and inner curve should be chosen closer to the unknown curve.
  - The conjugate gradient method is too slow for the Kirsch-Kress method. Advanced optimization schemes solve linear systems of equations which are larger than those of the direct solvers.
- Algorithms work also for domains with Jones modes.

References.

Uniqueness results:

D. Natroshvili, S. Kharibegashvili, and Z. Tediashvili, *Direct and inverse fluid-structure interaction problems*, Rend. Mat. Appl., VII Ser., Roma, **20** (2000), pp. 173–198.

P. Monk and V. Selgas, *An inverse fluid-solid interaction problem*, Inverse Problems and Imaging, **3** (2009), pp. 173–198.

Numerical schemes:

A.H. Barnett and T. Betcke, *Stabilty and convergence of the method of fundamental solutions for Helmholtz problems on analytic domains*, J. Comput. Physics, **227** (2008), pp. 7003–7026.

O. Ivanyshyn, R. Kress, and P. Serranho, *Huygens' principle and iterative methods in inverse obstacle scattering*, Advances Comput. Math., to appear.

J. Elschner, G.H. Hsiao, and A. R., *An Inverse Problem for Fluid-Solid Interaction*, Inverse Problems and Imaging, **2** (2008), pp. 83-120.

P. Monk and V. Selgas, *An inverse fluid-solid interaction problem*, Inverse Problems and Imaging, **3** (2009), pp. 173–198.

J. Elschner, G.H. Hsiao, and A. R., *An optimization method in inverse acoustic scattering by an elastic obstacle*, SIAM J. Appl. Math., **70** (2009), pp. 168–187.

J. Elschner, G.H. Hsiao, and A. R., *Comparison of numerical methods for the reconstruction of elastic obstacles from the far-field data of scattered acoustic waves*, WIAS-Preprint, **1479**, 2010.

Thank you for your attention!